J|A|C|S ARTICLES

Published on Web 06/04/2009

Storage of Hydrogen, Methane, and Carbon Dioxide in Highly Porous Covalent Organic Frameworks for Clean Energy Applications

Hiroyasu Furukawa* and Omar M. Yaghi*

Center for Reticular Chemistry, Department of Chemistry and Biochemistry, University of California—Los Angeles, Los Angeles, California 90095-1569

Received March 1, 2009; E-mail: furukawa@chem.ucla.edu; yaghi@chem.ucla.edu

Abstract: Dihydrogen, methane, and carbon dioxide isotherm measurements were performed at 1−85 bar and 77−298 K on the evacuated forms of seven porous covalent organic frameworks (COFs). The uptake behavior and capacity of the COFs is best described by classifying them into three groups based on their structural dimensions and corresponding pore sizes. Group 1 consists of 2D structures with 1D small pores (9 Å for each of COF-1 and COF-6), group 2 includes 2D structures with large 1D pores (27, 16, and 32 Å for COF-5, COF-8, and COF-10, respectively), and group 3 is comprised of 3D structures with 3D medium-sized pores (12 Å for each of COF-102 and COF-103). Group 3 COFs outperform group 1 and 2 COFs, and rival the best metal−organic frameworks and other porous materials in their uptake capacities. This is exemplified by the excess gas uptake of COF-102 at 35 bar (72 mg g^{-1} at 77 K for hydrogen, 187 mg g^{-1} at 298 K for methane, and 1180 mg g^{-1} at 298 K for carbon dioxide), which is similar to the performance of COF-103 but higher than those observed for COF-1, COF-5, COF-6, COF-8, and COF-10 (hydrogen at 77 K, 15 mg g^{-1} for COF-1, 36 mg g^{-1} for COF-5, 23 mg g^{-1} for COF-6, 35 mg g^{-1} for COF-8, and 39 mg g^{-1} for COF-10; methane at 298 K, 40 mg g^{-1} for COF-1, 89 mg g^{-1} for COF-5, 65 mg g^{-1} for COF-6, 87 mg g^{-1} for COF-8, and 80 mg g^{-1} for COF-10; carbon dioxide at 298 K, 210 mg g^{-1} for COF-1, 779 mg g^{-1} for COF-5, 298 mg g^{-1} for COF-6, 598 mg g^{-1} for COF-8, and 759 mg g^{-1} for COF-10). These findings place COFs among the most porous and the best adsorbents for hydrogen, methane, and carbon dioxide.

Introduction

Carbon dioxide emissions resulting from the burning of fossil fuels in automobiles and power plants is a pressing global environmental problem.[1] In the United States, approximately 20 metric tons of carbon dioxide per capita are released annually into the atmosphere.[1a,b] Carbon dioxide emissions contribute to global warming, sea level rise, and an irreversible increase in the acidity levels of the oceans with undesirable impact on the environment.[1c] We have undertaken several projects aimed at using hydrogen as a clean fuel for automobiles and producing clean energy by designing efficient systems to capture carbon dioxide. Additionally, we have a long-standing collaboration with BASF to expand the use of methane as an automobile fuel because it is significantly cleaner than petroleum.[2] In each of these cases there are several technical challenges (discussed below) to be overcome. We believe these can be addressed by employing highly porous materials as storage media. We[3−5] and others[6−8] have shown that metal−organic frameworks (MOFs) can be used to compact gases within the MOF pore structure. MOFs can achieve higher storage capacities for hydrogen,

(1) (a) Leaf, D.; Verolmec, H. J. H.; Hunt, W. F., Jr. *Environ. Int.* **2003**, *29*, 303–310. (b) Tucker, M. *Ecol. Econ.* **1995**, *15*, 215–223. (c) IPCC 2007. *Climate Change 2007: Synthesis Report*; Pachauri, R. K., Reisinger, A., Eds.; IPCC: Geneva, Switzerland, 2008.

(2) Jacoby, M. *Chem. Eng.* **2008**, *86* (Aug 25), 13–16.

(3) (a) Chen, B.; Ockwig, N. W.; Millward, A. R.; Contreras, D. S.; Yaghi, O. M. *Angew. Chem., Int. Ed.* **2005**, *44*, 4745–4749. (b) Wong-Foy, A. G.; Matzger, A. J.; Yaghi, O. M. *J. Am. Chem. Soc.* **2006**, *128*, 3494–3495. (c) Rowsell, J. L. C.; Yaghi, O. M. *J. Am. Chem. Soc.* **2006**, *128*, 1304–1315. (d) Furukawa, H.; Miller, M. A.; Yaghi, O. M. *J. Mater. Chem.* **2007**, *17*, 3197–3204.

(4) (a) Eddaoudi, M.; Kim, J.; Rosi, N.; Vodak, D.; Wachter, J.; O'Keeffe, M.; Yaghi, O. M. *Science* **2002**, *295*, 469–472. (b) Sudik, A. C.; Millward, A. R.; Ockwig, N. W.; Côté, A. P.; Kim, J.; Yaghi, O. M. *J. Am. Chem. Soc.* **2005**, *127*, 7110–7118.

(5) (a) Millward, A. R.; Yaghi, O. M. *J. Am. Chem. Soc.* **2005**, *127*, 17998–17999. (b) Walton, K. S.; Millward, A. R.; Dubbeldam, D.; Frost, H.; Low, J. J.; Yaghi, O. M.; Snurr, R. Q. *J. Am. Chem. Soc.* **2008**, *130*, 406–407.

(6) (a) Dincă, M.; Dailly, A.; Liu, Y.; Brown, C. M.; Neumann, D. A.; Long, J. R. *J. Am. Chem. Soc.* **2006**, *128*, 16876–16883. (b) Lin, X.; Jia, J.; Zhao, X.; Thomas, K. M.; Blake, A. J.; Walker, G. S.; Champness, N. R.; Hubberstey, P.; Schröder, M. *Angew. Chem., Int. Ed.* **2006**, *45*, 7358–7364. (c) Kaye, S. S.; Dailly, A.; Yaghi, O. M.; Long, J. R. *J. Am. Chem. Soc.* **2007**, *129*, 14176–14177. (d) Kesanli, B.; Cui, Y.; Smith, M. R.; Bittner, E. W.; Bockrath, B. C.; Lin, W. *Angew. Chem., Int. Ed.* **2005**, *44*, 72–75. (e) Panella, B.; Hirscher, M.; Pütter, H.; Müller, U. *Adv. Funct. Mater.* **2006**, *16*, 520–524. (f) Ma, S.; Sun, D.; Ambrogio, M.; Fillinger, J. A.; Parkin, S.; Zhou, H.-C. *J. Am. Chem. Soc.* **2007**, *129*, 1858–1859. (g) Chun, H.; Dybtsev, D. N.; Kim, H.; Kim, K. *Chem.—Eur. J.* **2005**, *11*, 3521–3529. (h) Chen, B.; Zhao, X.; Putkham, A.; Hong, K.; Lobkovsky, E. B.; Hurtado, E. J.; Fletcher, A. J.; Thomas, K. M. *J. Am. Chem. Soc.* **2008**, *130*, 6411–6423. (i) Wang, X.-S.; Ma, S.; Rauch, K.; Simmons, J. M.; Yuan, D.; Wang, X.; Yildirim, T.; Cole, W. C.; López, J. J.; de Meijere, A.; Zhou, H.-C. *Chem. Mater.* **2008**, *20*, 3145–3152. (j) Lin, X.; Telepeni, I.; Blake, A. J.; Dailly, A.; Brown, C. M.; Simmons, J. M.; Zoppi, M.; Walker, G. S.; Thomas, K. M.; Mays, T. J.; Hubberstey, P.; Champness, N. R.; Schröder, M. *J. Am. Chem. Soc.* **2009**, *131*, 2159–2171. (k) Panella, B.; Hirscher, M. *Adv. Mater.* **2005**, *17*, 358–541.

methane, and carbon dioxide than other porous materials such as zeolites and porous carbons.[9] In an effort to expand the realm of possibilities for materials that could be used in such clean energy applications, we recently reported the synthesis and structural characterization of a new class of porous frameworks termed covalent organic frameworks (COFs).[10,11] Unlike MOFs, COF structures are entirely composed of light elements (H, B, C, and O) that are linked by strong covalent bonds (B−O, C−C, and B−C) to make a highly porous class of materials. Indeed, one member of this class has the lowest density ever reported for a crystalline solid (0.17 g cm^{-3} for COF-108).[10b] This has led us to investigate the potential use of COFs in the storage of some gases relevant to clean energy. Here we report the first adsorption studies of hydrogen, methane, and carbon dioxide in COFs and show that COFs rank among the highest performing materials in terms of their gas storage capacities.

Experimental Section

Synthesis of Compounds. Crystalline samples of the as-synthesized forms of the compounds COF-1, -5, -6, -8, -10, -102, and -103 were obtained using published procedures.[10] Briefly, 2,3,6,7,10,11-hexahydroxytriphenylene (HHTP) and 1,4-benzenediboronic acid (BDBA) were purchased from TCI and Aldrich, respectively. 1,3,5-Tris[(4-dihydroxyboryl)phenyl]benzene (TBPA), 4,4′-biphenyldiboronic acid (BPDA), and 1,3,5-benzenetriboronic acid (BTBA) were prepared according to modifications of published procedures.[12] Tetra(4-(dihydroxy)borylphenyl)silane (TBPS) and tetra(4-(dihydroxy)borylphenyl)methane (TBPM) were prepared according to literature methods.[13] Mesitylene (98%, Fluka) and anhydrous 1,2-dioxane (99.8%, Aldrich) were used for the condensation reactions. Typically for the synthesis of COF materials, the reaction mixture [i.e., boronic acid and HHTP in mesitylene/dioxane (1:1, v/v)] was heated at 85 °C for several days to afford microcrystalline solids. Their identity was confirmed using elemental microanalysis, thermal gravimetric analysis, FT-IR spectroscopy, and powder X-ray diffraction.[10]

Low-Pressure Gas Adsorption Measurements. Low-pressure N_2, Ar, H_2, CH_4, and CO_2 adsorption measurements (up to 1 bar) were performed on an Autosorb-1 (Quantachrome) volumetric analyzer.[3d] The adsorption data were measured using a volumetric technique that represents excess adsorption isotherms. The samples were outgassed to 10^{-6} Torr. Helium was used for the estimation of the dead volume, assuming that it is not adsorbed at any of the studied temperatures. Liquid nitrogen, liquid argon, and ice/water baths were used for adsorption measurements at 77, 87, and 273 K, respectively. To provide high accuracy and precision in determining P/P_0, the saturation pressure P_0 was measured throughout the N_2 and Ar analyses by means of a dedicated saturation pressure transducer, which allowed us to monitor the vapor pressure for each data point. Ultra-high-purity grade Ar, N_2, H_2, CH_4, He (99.999% purity), and CO_2 gases (99.995% purity) were used throughout the adsorption experiments. Nonideality of gases was obtained from the second virial coefficient at experimental temperature.[14]

Gravimetric High-Pressure Gas Adsorption Measurements. Gravimetric gas adsorption isotherms were measured on a GHP-300 gravimetric high-pressure analyzer from VTI Corp. (currently TA Instruments).[3d] A Rubotherm magnetic suspension balance (MC-5) was used to measure the change in mass of samples suspended within a tube (22 mm i.d.) constructed from Inconel 625 under a chosen atmosphere. Prior to admittance of the analyte gas, the entire chamber and manifold were evacuated at room temperature, and the weight of the Al sample bucket (12 mm i.d. × 21 mm length) was measured. After loading of COF samples (200−400 mg), the system was purged at room temperature with helium, and the sample was outgassed, using a turbomolecular drag pump (Pfeiffer, TSH 071 E), until a constant mass was attained. When H_2 gas was used, water and other condensable impurities were removed with a liquid nitrogen trap. The pressure was measured with an MKS Baratron transducer 120AA (0−1000 Torr) and an electronic Bourdon gauge-type transducer (Mensor, up to 1500 psi). The adsorbate was added incrementally, and data points were recorded when no further change in mass was observed. The temperature in the Inconel tube was also monitored with a platinum resistance thermometer.

To obtain the excess adsorption isotherm, all data points were corrected for buoyancy and the thermal gradient that arises between the balance (313 K) and the sample bucket. Buoyancy and thermal-gradient effects exhibited by the bucket and the components associated with the magnetic-suspension balance were corrected on the basis of the change in mass of the empty bucket within the analyte gas at experimental temperature. The weight loss due to the buoyancy of the adsorbent was determined by multiplying the volume of COF framework skeleton (i.e., backbone density, d_{bb})

(7) (a) Seki, K.; Mori, W. *J. Phys. Chem. B* **2002**, *106*, 1380–1385. (b) Noro, S.; Kitagawa, S.; Kondo, M.; Seki, K. *Angew. Chem., Int. Ed.* **2000**, *39*, 2081–2084. (c) Kitaura, R.; Seki, K.; Akiyama, G.; Kitagawa, S. *Angew. Chem., Int. Ed.* **2003**, *42*, 428–431. (d) Bourrelly, S.; Llewellyn, P. L.; Serre, C.; Millange, F.; Loiseau, T.; Férey, G. *J. Am. Chem. Soc.* **2005**, *127*, 13519–13521. (e) Surblé, S.; Millange, F.; Serre, C.; Düren, T.; Latroche, M.; Bourrelly, S.; Llewellyn, P. L.; Férey, G. *J. Am. Chem. Soc.* **2006**, *128*, 14889–14896. (f) Llewellyn, P. L.; Bourrelly, S.; Serre, C.; Vimont, A.; Daturi, M.; Hamon, L.; De Weireld, G.; Chang, J.-S.; Hong, D.-Y.; Hwang, Y. K.; Jhung, S. H.; Férey, G. *Langmuir* **2008**, *24*, 7245–7250. (g) Loiseau, T.; Lecroq, L.; Volkringer, C.; Marrot, J.; Férey, G.; Haouas, M.; Taulelle, F.; Bourrelly, S.; Llewellyn, P. L.; Latroche, M. *J. Am. Chem. Soc.* **2006**, *128*, 10223–10230. (h) Ma, S.; Sun, D.; Simmons, J. M.; Collier, C. D.; Yuan, D.; Zhou, H.-C. *J. Am. Chem. Soc.* **2008**, *130*, 1012–1016. (i) Zhou, W.; Wu, H.; Hartman, M. R.; Yildirim, T. *J. Phys. Chem. C* **2007**, *111*, 16131–16137.

(8) (a) Chen, B.; Ma, S.; Zapata, F.; Fronczek, F. R.; Lobkovsky, E. B.; Zhou, H.-C. *Inorg. Chem.* **2007**, *46*, 1233–1236. (b) Kondo, A.; Noguchi, H.; Ohnishi, S.; Kajiro, H.; Tohdoh, A.; Hattori, Y.; Xu, W.-C.; Tanaka, H.; Kanoh, H.; Kaneko, K. *Nano Lett.* **2006**, *6*, 2581–2584.

(9) (a) Ströbel, R.; Garche, J.; Moseley, P. T.; Jörissen, L.; Wolf, G. *J. Power Sources* **2006**, *159*, 781–801. (b) Bénard, P.; Chahine, R. *Langmuir* **2001**, *17*, 1950–1955. (c) Texier-Mandoki, N.; Dentzer, J.; Piquero, T.; Saadallah, S.; David, P.; Vix-Guterl, C. *Carbon* **2004**, *42*, 2744–2747. (d) Nijkamp, M. G.; Raaymakers, J. E. M. J.; van Dillen, A. J.; de Jong, K. P. *Appl. Phys. A: Mater. Sci. Process.* **2001**, *72*, 619–623. (e) Langmi, H. W.; Book, D.; Walton, A.; Johnson, S. R.; Al-Mamouri, M. M.; Speight, J. D.; Edwards, P. P.; Harris, I. R.; Anderson, P. A. *J. Alloys Compd.* **2005**, *404−406*, 637–642. (f) Yang, Z.; Xia, Y.; Mokaya, R. *J. Am. Chem. Soc.* **2007**, *129*, 1673–1679. (g) Wood, C. D.; Tan, B.; Trewin, A.; Niu, H.; Bradshaw, D.; Rosseinsky, M. J.; Khimyak, Y. Z.; Campbell, N. L.; Kirk, R.; Stockel, E.; Cooper, A. I. *Chem. Mater.* **2007**, *19*, 2034–2048. (h) Ghanem, B. S.; Msayib, K. J.; McKeown, N. B.; Harris, K. D. M.; Pan, Z.; Budd, P. M.; Butler, A.; Selbie, J.; Book, D.; Walton, A. *Chem. Commun.* **2007**, 67–69. (i) Germain, J.; Hradil, J.; Fréchet, J. M. J.; Svec, F. *Chem. Mater.* **2006**, *18*, 4430–4435.

(10) (a) Côté, A. P.; Benin, A. I.; Ockwig, N. W.; O'Keeffe, M.; Matzger, A. J.; Yaghi, O. M. *Science* **2005**, *310*, 1166–1170. (b) El-Kaderi, H. M.; Hunt, J. R.; Mendoza-Cortés, J. L.; Côté, A. P.; Taylor, R. E.; O'Keeffe, M.; Yaghi, O. M. *Science* **2007**, *316*, 268–272. (c) Côté, A. P.; El-Kaderi, H. M.; Furukawa, H.; Hunt, J. R.; Yaghi, O. M. *J. Am. Chem. Soc.* **2007**, *129*, 12914–12915.

(11) (a) Tilford, R. W.; Gemmil, W. R.; zur Loye, H.-C.; Lavigne, J. J. *Chem. Mater.* **2006**, *18*, 5296–5301. (b) Tilford, R. W.; Mugavero, S. J.; Pellechia, P. J.; Lavigne, J. J. *Adv. Mater.* **2008**, *20*, 2741–2746. (c) Hunt, J. R.; Doonan, C. J.; LeVangie, J. D.; Côté, A. P.; Yaghi, O. M. *J. Am. Chem. Soc.* **2008**, *130*, 11872–11873. (d) Wan, S.; Guo, J.; Kim, J.; Ihee, H.; Jiang, D. *Angew. Chem., Int. Ed.* **2008**, *47*, 8826–8830.

(12) (a) Morgan, A. B.; Jurs, J. L.; Tour, J. M. *J. Appl. Polym. Sci.* **2000**, *76*, 1257–1268. (b) Goldschmid, H. R.; Musgrave, O. C. *J. Chem. Soc. C* **1970**, 488–493.

(13) Fournier, J.-H.; Maris, T.; Wuest, J. D.; Guo, W.; Galoppini, E. *J. Am. Chem. Soc.* **2003**, *125*, 1002–1006.

(14) Dymond, J. H.; Smith, E. B. *The Virial Coefficients of Pure Gases and Mixtures*; Clarendon Press: Oxford, 1980.

Table 1. Summary of Porosity Measurements for COFs and Other Porous Materials[a]

material	composition	pore size/Å	S_{Lang}/ $m^2\ g^{-1}$	S_{BET}/ $m^2\ g^{-1}$	$V_{p,DR}$/ $cm^3\ g^{-1}$	d_{bulk}/ $g\ cm^{-3}$	d_{bb}/ $g\ cm^{-3}$	Q_{st}/ $kJ\ mol^{-1}$	H_2 uptake/ $mg\ g^{-1}$	CH_4 uptake/ $mg\ g^{-1}$	CO_2 uptake/ $mg\ g^{-1}$
COF-1	C_3H_2BO	9	970	750	0.30	0.98	1.39	6.2	14.8	40 (44)	230
COF-5	$C_9H_4BO_2$	27	1990 (3300)	1670 (2050)	1.07	0.58	1.57	6.0	35.8	89 (127)	870
COF-6	$C_8H_3BO_2$	9	980	750	0.32	1.1	1.71	7.0	22.6	65 (68)	310
COF-8	$C_{14}H_7BO_2$	16	1400 (2110)	1350 (1710)	0.69	0.71	1.32	6.3	35.0	87 (114)	630
COF-10	$C_{12}H_6BO_2$	32	2080 (4620)	1760 (1980)	1.44	0.48	1.56	6.6	39.2	80 (124)	1010
COF-102	$C_{25}H_{24}B_4O_8$	12	4650	3620	1.55	0.43	1.32	3.9	72.4	187 (243)	1200
COF-103	$C_{24}H_{24}B_4O_8Si$	12	4630	3530	1.54	0.43	1.29	4.4	70.5	175 (229)	1190
BPL carbon			1500	1250	0.56	0.87	2.13	8.0	25.5	86 (94)	370
zeolites				260−590[29]	0.20−0.36[29]					31−82[29]	220−350[52]
mesoporous silicas				450−1070[29]		0.17−0.45[29]				14−65[29]	
Maxsorb				3100[29]		0.37[29]				211[29]	
anthracite				3300[42]						250 (at 293 K)[42]	
Norit RB2			1180[5a]								420 (40 bar)[5a]
MOF-5 (IRMOF-1)	$C_{24}H_{12}O_{13}Zn_4$	12, 15	4400[6c]	3800[6c]		0.59[3b]		4.8[3c]	76[6c]	120 (at 300 K)[7i]	970 (40 bar)[5a]
MOF-177	$C_{54}H_{30}O_{13}Zn_4$	11, 17	5640[3b]	4750[3b]		0.43[3b]		4.4[3d]	75.2[3b]		1490 (40 bar)[5a]
IRMOF-6	$C_{30}H_{18}O_{13}Zn_4$	10, 15	3310[3b]	2800[3b]		0.65[3b]			48.5[3b]	160[4a]	870 (40 bar)[5a]
Cu-MOF	$C_{17}H_{14}O_4NCu$	11		3270[7a]	1.26[7a]					160[7a]	
PCN-14	$C_{15}H_9O_5Cu$	8	2180[7h]	1750[7h]	0.87[7h]	0.83[7h]				253 (at 290 K)[7h]	
MIL-101(Cr)	$C_{24}H_{12}O_{13}FCr$	29, 34		4230[7f]	2.15[7f]	0.44[7f]				160[7f]	1760 (50 bar)[7f]

[a] S_{Lang} and S_{BET} are the Langmuir and BET surface areas. The surface areas in parentheses are calculated on the basis of the second step of the adsorption branch. $V_{p,DR}$ is the measured total pore volume. d_{bulk} and d_{bb} are the bulk density and the backbone density of materials. Q_{st} is the isosteric heat of adsorption for H_2 at zero coverage. H_2 uptake is the saturation H_2 uptake at 77 K. CH_4 and CO_2 uptakes are those at 35 and 55 bar, respectively, and 298 K. The CH_4 uptakes in parentheses are the uptakes at 85 bar and 298 K.

times the density of H_2 (i.e., corrected mass for buoyancy is $V_{bb} \times \rho_{bulk}$).[15] The volume of COF framework skeleton was determined from the helium (<10 bar) buoyancy curve at 298 K using the same gravimetric system.[3d,16] The absolute amount of gas adsorbed was calculated from the density of the framework skeleton (an inverse of the skeleton volume) and the crystallographic density, leading to an accessible pore volume for the samples.

Estimation of Bulk Density. By use of d_{bb} and d_{bulk}, available based on modeling of COF structures, the accessible pore volume ($V_{p,He}$) was calculated from the following equation: $V_{p,He} = 1/d_{bulk} - 1/d_{bb}$. Ideally, the $V_{p,He}$ should be comparable to the pore volume from low-pressure Ar or N_2 isotherms using the Dubinin−Radushkevich (DR) method ($V_{p,DR}$), if the pore aperture and diameter are large enough for guest diffusion and storage. Indeed, for many of the MOFs, $V_{p,He}$ is consistent with $V_{p,DR}$.[17,18] However, obvious deviation from this ideal relationship was observed for COF-1, -6, -10, -102, and -103.[19] Therefore, in this contribution, pore volumes from the DR plots were used for COF-1, -6, -10, -102, and -103 samples, and their bulk densities were recalculated using the experimental pore volumes ($V_{p,DR}$) and densities [$d_{bulk} = 1/(V_{p,DR} + 1/d_{bb})$]. For the remaining COFs, V_p values from He isotherms were used, and the values of d_{bb} are listed in Table 1. Note that this process has no impact on high-pressure gas adsorption data (surface excess amount), and the corrected bulk density was used for estimation of absolute uptake in volumetric units (g L^{-1}).[20]

Results and Discussion

Description of COF Structures. We briefly describe the crystal structures of the materials we synthesized and studied (Figure 1). COF-1 was synthesized by self-condensation reactions of BDBA.[10a] The building units produce a planar six-membered B_3O_3 ring with the elimination of three water molecules. COF-5, -6, -8, and -10 were obtained through co-condensation reactions of HHTP with BDBA, BTBA, TBPA, and BPDA, respectively.[10a,c] In each case, a five-membered C_2O_2B ring in the trigonal HHTP boronate ester is formed by the dehydration reaction. With the exception of COF-1, where the layers are staggered as in graphite (**gra**[20]), the 2D COFs form an eclipsed layered structure as in α-BN (**bnn**) with 1D channels of varying size (Table 1).[10a,c]

Crystalline forms COF-102 and -103 are prepared by self-condensation reactions of TBPM and TBPS (Figure 1).[10b] Dehydration reaction of TBPM and TBPS produces a B_3O_3 ring, which can be considered to be a triangular node. From the combination of triangular and tetrahedral nodes (with C or Si atom in the link), a structure based on the hypothetical carbon nitride C_3N_4 (**ctn**) is obtained.

For easy reference, the aforementioned COFs are classified into three groups depending on the dimensionality of the structure and the corresponding pore size: group 1, 2D structures with 1D small pores (9 Å for each of COF-1 and -6); group 2, 2D structures with large 1D pores (27, 16, and 32 Å for COF-5, -8, and -10, respectively); and group 3, 3D structures with

(15) Ideally, the buoyancy correction for adsorbed guests should be performed. However, the adsorbate density and the density profiles in the pore cannot be measured by today's technology.[3d] In this contribution, we assume that the adsorbate volume is negligible.[17]

(16) Murata, K.; Kaneko, K.; Kokai, F.; Takahashi, K.; Yudasaka, M.; Iijima, S. *Chem. Phys. Lett.* **2000**, *331*, 14–20.

(17) See Supporting Information for details.

(18) Pore volumes from N_2 isotherms also show a good correlation; however, we recommend the use of Ar isotherms because Ar is a spherical molecule and interaction with the adsorbent is weaker than for N_2.

(19) Although there are several possible explanations, including contamination of solvents or impurities, the main reason for this discrepancy may be the partial decomposition of materials resulting in underestimation of bulk density. If the compound is partially decomposed, the experimental bulk density should be larger than calculated crystal density.

(20) It is worth noting that comparison of two pore volumes determined by different methods is useful from a diagnostic point of view because if the material is not fully activated it leads to deviations in surface areas.[6c,k,7e] We note that successful sample activation should be confirmed by He isotherms.

(21) We use the symbols (bold) of the RCSR database (www.rcsr.anu.edu.au): O'Keeffe, M.; Peskov, M. A.; Ramsden, S. J.; Yaghi, O. M. *Acc. Chem. Res.* **2008**, *41*, 1782–1789.

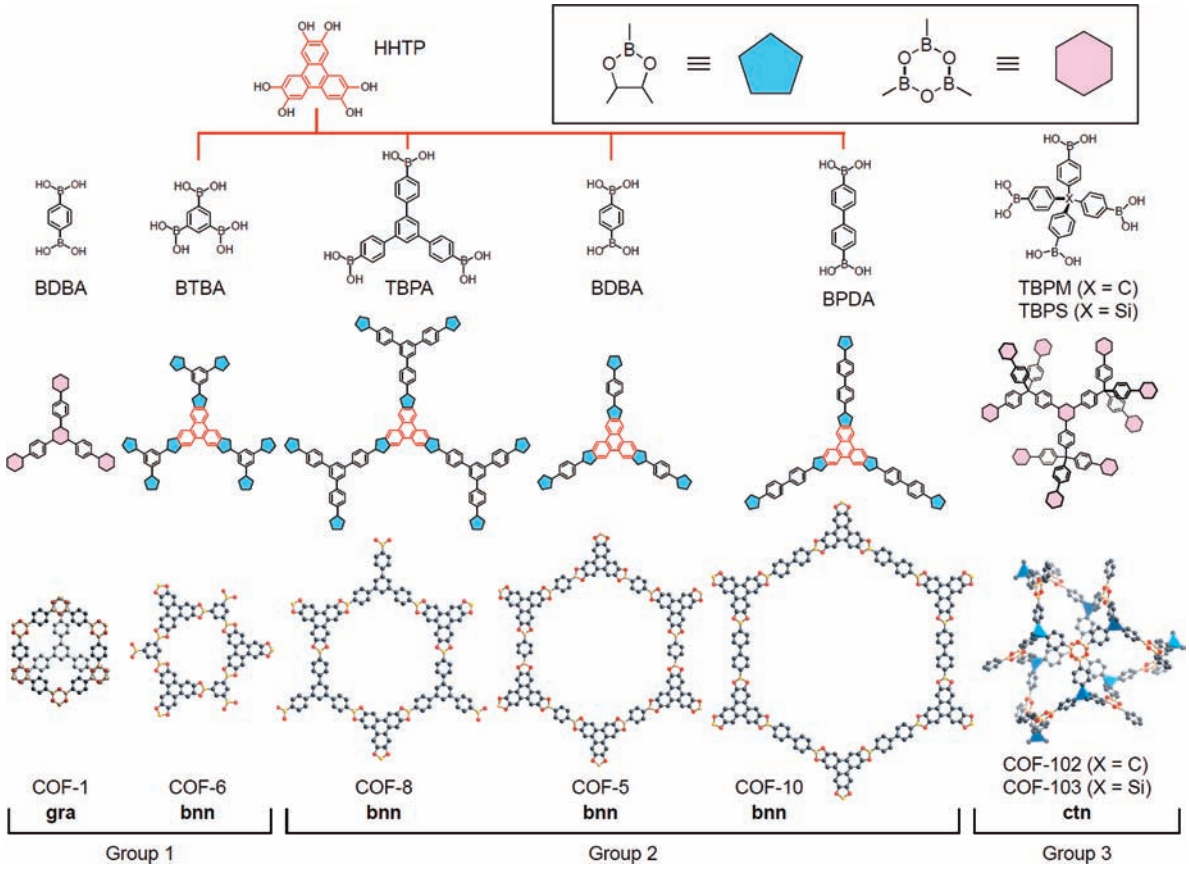

Figure 1. Condensation reactions of boronic acids and HHTP used to produce COFs (top), and resulting fragments of the COFs (middle). (bottom) Atomic connectivity and structure of crystalline products of 2D (COF-1, -5, -6, -8, and -10) and 3D (COF-102 and -103) COFs. B, orange; O, red; C, black; atom X in COF-102 and -103, blue tetrahedron; all hydrogen atoms are omitted for clarity. Inset: the C_2O_2B (blue) and the B_3O_3 (pink) rings formed by condensation reactions. The topology and the group classification number are indicated for each COF.

3D medium pores (12 Å for each of COF-102 and -103) (Figure 1 and Table 1).

Permanent Porosity of COFs. Table 1 summarizes the composition, metric pore data, results of adsorption measurements, and uptake capacities for each of the COF materials. Relevant data are also shown for state-of-the-art materials including porous carbon, zeolites, and MOFs. The framework stability and porosity of COFs were confirmed by evacuating the pores of the as-synthesized compounds at 10^{-6} Torr and measuring the Ar gas adsorption isotherm of the guest-free (activated) materials. Figure 2 shows the Ar isotherms measured for each of the COFs. The isotherms of group 1 COFs (COF-1 and -6) follow a classical type I behavior indicative of permanent microporosity. However, for group 2 COFs (COF-5, -8, and -10), a type IV behavior is observed, while for group 3 COFs (COF-102 and -103) a steep rise in Ar uptake is seen at approximately $P/P_0 = 1.5 \times 10^{-2}$, accompanied by unusual steps in the very low pressure region (Figure 2, log scale). In general, the amount of gas molecules adsorbed at a given pressure is influenced by adsorbent−adsorbate and adsorbate−adsorbate interactions; thus, the differences in the isotherm profiles provide insight into the pore structures. The group 1 COFs display a sigmoidal-shaped Ar uptake profile (see log scale) followed by saturation in the range $P/P_0 = 10^{-4}-10^{-3}$, which corresponds to strong adsorption of Ar into the pores and subsequent pore-filling as typically observed in small-pore zeolites such as ZSM-5.[22] Such isotherm behavior suggests that the micropore filling in the group 1 COFs is substantially attributed to the overlapping potential from the walls of the framework.[23]

The pressure range of micropore filling increases with an increase in pore diameter of COFs, as observed in group 2 COFs. Here, the relative pressure for monolayer formation is observed in the lower range $P/P_0 = 5 \times 10^{-3}-1 \times 10^{-1}$ because these COFs have larger pores and therefore lower adsorption potentials. Indeed, in group 2 COFs, significant steps at $P/P_0 = 4.0 \times 10^{-2}$, 1.6×10^{-1}, and 2.8×10^{-1} for COF-8, -5, and -10, respectively, are observed because of multilayer formation and condensation.[10a,c] The fact that no significant hysteresis is observed in these isotherms is in agreement with a general trend that hysteresis due to capillary condensation should be observed only in materials with pores larger than 40 Å.[24]

For group 3 COFs, the shapes of the isotherms are unique and do not correspond to any of the IUPAC classification of gas adsorption isotherms.[23] In addition to the expected large step at $P/P_0 = 1.5 \times 10^{-2}$, which is attributed to pore-filling, an unusually small step at $P/P_0 = 5 \times 10^{-3}$ is found (Figure 2, log scale). This feature was also observed in the N_2 isotherms

(22) Storck, S.; Bretinger, H.; Maier, W. F. *Appl. Catal., A* **1998**, *174*, 137–146.
(23) Rouquerol, F.; Rouquerol, J.; Sing, K. *Adsorption by Powders & Porous Solids*; Academic Press: London, UK, 1999.
(24) Thommes, M.; Köhn, R.; Fröba, M. *Appl. Surf. Sci.* **2002**, *196*, 239–249.

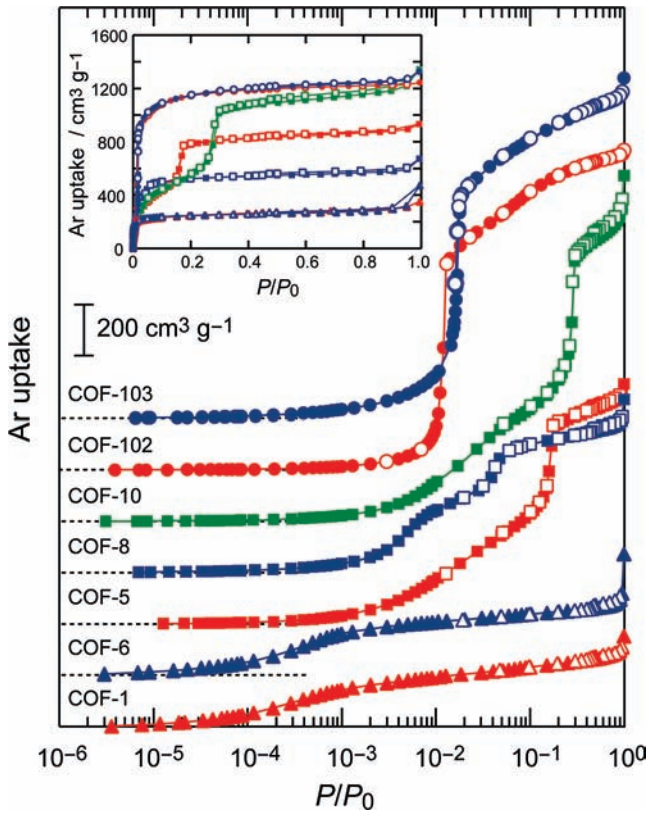

Figure 2. Ar isotherms for COFs measured at 87 K on a semilogarithmic scale. Adsorption data are shown as closed symbols and desorption data as open symbols; connecting traces are guides for the eye. (Inset) Ar isotherms for COFs are shown on a linear scale.

of these COFs (Supporting Information, Figures S7 and S8)[17] and was previously encountered in high-surface-area MOFs, such as MOF-5 and MOF-177.[3d,25] We learned from single-crystal X-ray diffraction studies of Ar and N_2 gases in MOFs that the metal oxide joints act as strong binding pockets within the pores and thus may be responsible for the appearance of such unusual steps.[25c] We believe that the Si(C) tetrahedral corners in group 3 COFs also act as strong binding sites for gases. A similar adsorption mechanism was proposed on the basis of simulation calculations for MOFs.[26]

From the Ar adsorption isotherms, the apparent surface area (Langmuir model) and total pore volume of each material have been calculated (Table 1). The pore volume of each material was estimated from the DR model with the assumption that the adsorbate is in the liquid state and the adsorption involves a pore-filling process. The BET surface areas (accessible surface area) for COFs are also presented in Table 1. We believe that the BET surface areas, rather than the pore volumes or apparent surface areas, represent more closely the actual surface areas in COFs, as the adsorbate−adsorbate interactions are significantly weaker than adsorbate−adsorbent physisorption in supercritical gases.[26] It is clear from Table 1 that COFs are among the most highly porous materials, in that their surface areas are within the range of ultrahigh surface areas found for MOFs.

Hydrogen Storage in COFs. For mobile fueling applications, at least 4 kg of hydrogen must be stored to allow a vehicle to drive a distance greater than several hundred kilometers before refueling.[27] The volume of 4 kg of H_2 gas corresponds to 50 000 L at room temperature and ambient pressure. In order to achieve practical compact fuel cell systems, the storage issues associated with the high volumetric and gravimetric density of hydrogen must be addressed. Two basic approaches have emerged to achieve the targets for on-board H_2 storage systems set by the U.S. Department of Energy (DOE): 6.0 wt % and 45 g of H_2 L^{-1} by the year 2010. One is to chemisorb H_2 as metal hydrides or chemical hydrides.[28] Although some metal hydrides are able to meet the DOE target for H_2 storage capacity,[27] their high discharge temperature and poor cycle performance remain roadblocks to their successful implementation in real-world systems. The other approach is to physisorb H_2 in porous materials such as carbon-based materials, zeolites, polymers, and MOFs.[3,6,9,29] Several MOFs and porous carbon materials with high surface area meet the 2010 DOE targets at 77 K; however, significant room temperature uptake remains a challenge. One of the reasons for the diminished storage capacity at room temperature is the weak adsorbent−H_2 interaction due to the lack of strong binding sites. Recently, the simulation of H_2 uptake behavior in COFs by several groups[30] has led to the prediction that some COFs store greater amounts of H_2 than MOFs. The low-pressure H_2 isotherms of COFs measured at 77 K are shown in Figure 3a. The rapid pressure equilibration and absence of hysteresis confirm that H_2 is reversibly physisorbed.[31] Under these conditions, H_2 isotherms are not fully saturated because of the low critical temperature of H_2 (33 K).[32] The uptake of H_2 in the low-pressure region does not depend on either the surface area or the pore volume of the compounds;[33] however, characteristic H_2 uptake behavior can be seen, as there is a difference in the adsorption enthalpy of H_2 among the selected COFs (Figure 3b). The coverage dependencies of H_2−COF interactions (isosteric heat of adsorption, Q_{st}) were calculated on the basis of the H_2 isotherms recorded at 77 and 87 K, as shown in Figure 3a and Figures S9−S16 in the Supporting Information, respectively, and as summarized in Table 1. The Q_{st} curve for BPL carbon is included as a reference.[3c,d,34]

Within group 1 materials, COF-1 shows a gradual, nearly linear decrease in its Q_{st} value as a function of the amount of H_2 adsorbed, while COF-6 has larger Q_{st} values below a surface H_2 coverage of 2 mg g^{-1} and subsequent linear decrease with

(25) (a) Li, H.; Eddaoudi, M.; O'Keeffe, M.; Yaghi, O. M. *Nature* **1999**, *402*, 276–279. (b) Chae, H. K.; Siberio-Pérez, D. Y.; Kim, J.; Go, Y.-B.; Eddaoudi, M.; Matzger, A. J.; O'Keeffe, M.; Yaghi, O. M. *Nature* **2004**, *427*, 523–527. (c) Rowsell, J. L. C.; Spencer, E. C.; Eckert, J.; Howard, J. A. K.; Yaghi, O. M. *Science* **2005**, *309*, 1350–1354.
(26) Walton, K. S.; Snurr, R. Q. *J. Am. Chem. Soc.* **2007**, *129*, 8552–8556.
(27) (a) Satyapal, S.; Petrovic, J.; Read, C.; Thomas, G.; Ordaz, G. *Catal. Today* **2007**, *120*, 246–256. (b) Felderhoff, M.; Weidenthaler, C.; von Helmolt, R.; Eberle, U. *Phys. Chem. Chem. Phys.* **2007**, *9*, 2643–2653.
(28) (a) Orimo, S.; Nakamori, Y.; Eliseo, J. R.; Züttel, A.; Jensen, C. M. *Chem. Rev.* **2007**, *107*, 4111–4132. (b) Struzhkin, V. V.; Militzer, B.; Mao, W. L.; Mao, H.-K.; Hemley, R. J. *Chem. Rev.* **2007**, *107*, 4133–4151. (c) Solan, E. D. *Nature* **2003**, *426*, 353–359. (d) Lee, H.; Lee, J.-W.; Kim, D. Y.; Park, J.; Seo, Y.-T.; Zeng, H.; Moudrakovski, I. L.; Ratcliffe, C. I.; Ripmeester, J. A. *Nature* **2005**, *434*, 743–746.
(29) Menon, V. C.; Komarneni, S. *J. Porous Mater.* **1998**, *5*, 43–58.
(30) (a) Han, S. S.; Furukawa, H.; Yaghi, O. M.; Goddard, W. A. *J. Am. Chem. Soc.* **2008**, *130*, 11580–11581. (b) Klontzas, E.; Tylianakis, E.; Froudakis, G. E. *J. Phys. Chem. C* **2008**, *112*, 9095–9098.
(31) Li, Y.; Yang, R. T. *AIChE J.* **2008**, *54*, 269–279.
(32) Thermophysical properties of fluid systems. NIST Chemistry Webbook, http://webbook.nist.gov/chemistry/fluid/.
(33) Frost, H.; Düren, T.; Snurr, R. Q. *J. Phys. Chem. B* **2006**, *110*, 9565–9570.
(34) (a) Czepirski, L.; Jagiello, J. *Chem. Eng. Sci.* **1989**, *44*, 797–801. (b) Jagiello, J.; Bandosz, T. J.; Putyera, K.; Schwarz, J. A. *J. Chem. Eng. Data* **1995**, *40*, 1288–1292.

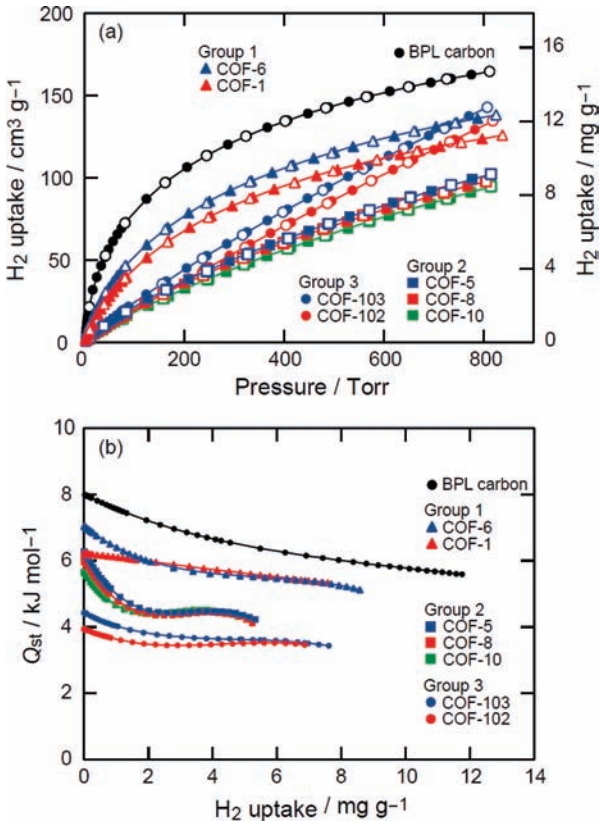

Figure 3. (a) Low-pressure H_2 isotherms for COFs measured at 77 K and (b) coverage dependency of adsorption enthalpies for COFs. Data for BPL carbon are shown for comparison.

increasing amounts of adsorbed H_2. Considering that the pore diameters of COF-1 and COF-6 are analogous, the difference in the Q_{st} traces may be attributed to the stacking motifs of their layers. In COF-6 the small striations in the eclipsed stacking of layers are available to adsorb H_2 with greater enthalpic gain; once these sites are occupied, adsorption onto other sites is less energetically favorable.[10c] This result is consistent with the results obtained for group 2 materials, COF-5, -8, and -10, whose Q_{st} values also decrease and become flat at a surface coverage of 2 mg g^{-1}. It is noteworthy that the Q_{st} values for the group 2 materials are similar despite the fact that their corresponding pore diameters are different, an observation which suggests the lack of the effective energy of adsorption as is generally provided by narrow micropores.[23,35] Group 3 COFs display the lowest isosteric heat of adsorption over the whole range of coverage measured. Here, the gradual decrease in the Q_{st} values suggests that the number of strong binding sites is not high in these structures, as observed for MOF-177 and MOF-5 (Table 1).[3c,d] The coverage dependence of Q_{st} for group 3 COFs is characteristic of highly porous materials. In other words, an adsorption pocket (or corrugated surface) should be preferable for H_2 adsorption at 77 K in the low-pressure region rather than either flat surfaces or edges.

The saturation hydrogen uptake capacities in a series of COFs were evaluated by high-pressure gravimetric adsorption measurements. All data were corrected for the buoyancy of the system, adsorbents, and analytes. Isotherms acquired at 77 K

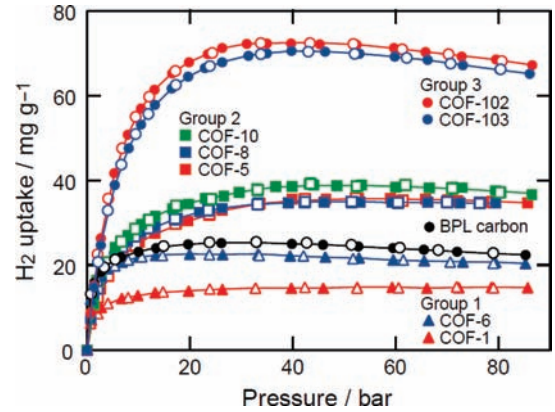

Figure 4. High-pressure H_2 isotherms for COFs measured at 77 K. Data for BPL carbon are shown for comparison.

are shown in Figure 4. The reversible isotherms and rapid pressure equilibration (ca. 5 min/step) indicate that H_2 is physisorbed even in the high-pressure region. Saturation uptakes vary widely: 14.8 and 22.6 mg g^{-1} for group 1 COFs, 35.8, 35.0, and 39.2 mg g^{-1} for group 2 COFs, and 72.4 and 70.5 mg g^{-1} for group 3 COFs. The saturation pressure of these isotherms increases with an increase in pore diameter. The same trends were reported for high-pressure H_2 adsorption in MOFs (Table 1).[3b] It is worth noting that the surface excess mass for COF-102, whose uptake is the highest in a series of COFs, is comparable to those of MOF-177 (75 mg g^{-1}) and MOF-5 (76 mg g^{-1}), although the saturation pressure for COF-102 is lower than for those MOFs.[3b,6c] This indicates that the pore size distribution of COF-102 is preferable to that of MOFs for H_2 adsorption and that the chemical composition of adsorbents is not always important for H_2 storage under these conditions.

Although the surface excess mass is a useful concept, the total amount that a material can store is more relevant to the practicability of using H_2 as a fuel. The total adsorbed amount of H_2 cannot be measured experimentally; however, we can estimate this value by using a knowledge of the COF pore volume and bulk H_2 density ($N_{abs} = N_{ex} + \rho_{bulk}V_{p,DR}$).[3d] In the high-pressure region, the bulk density of H_2 is not negligible and the amounts of H_2 corresponding to the second term ($\rho_{bulk}V_{p,DR}$) can reach 30−40% of the total H_2 uptake. Estimated absolute adsorbed amounts of H_2 are plotted in both volumetric and gravimetric uptake units as shown in Figure 5, which reveals a nearly linear correspondence (red circles), even though the variation in volumetric units is smaller than that in gravimetric units. These data suggest that a substantially larger pore volume is required to improve volumetric uptake capacities. In Figure 5, the H_2 uptake capacities for COFs are also compared to those of other representative materials, such as hydrocarbons, MOFs, and metal hydrides. Significantly, most of the compounds that display high volumetric H_2 density are hydrocarbons and alcohols, but such materials cannot release H_2 molecules reversibly. Chemical and complex metal hydrides such as $NaBH_4$ and $NaAlH_4$ exhibit high volumetric density of H_2; they have been investigated as potential H_2 storage materials.[28a] Some metal hydrides can release H_2 at desirable temperatures; however, irreversible H_2 release and poor cycle performance remain significant problems for these materials.[27b] Therefore, we believe that physisorptive materials which can operate near room temperature (large Q_{st}) must pursued,[36] in spite of the

(35) Lowell, S.; Shields, J. E.; Thomas, M. A.; Thommes, M. *Characterization of Porous Solids and Powders: Surface Area, Pore Size and Density*; Kluwer Academic Publishers: Dordrecht, 2004.

(36) Bhatia, S. K.; Myers, A. L. *Langmuir* **2006**, *22*, 1688–1700.

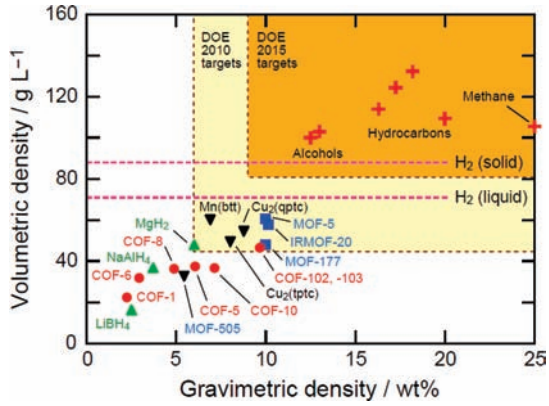

Figure 5. Stored H_2 per mass and per volume. Physisorbed H_2 density at 77 K in COFs and MOFs is shown, based on the absolute adsorbed amounts of H_2. The original data for MOFs were from refs 3 and 6. For hydride compounds, the value represents reversible H_2 uptake and release despite discharge temperature.[28a] H_2 density for hydrocarbons and alcohols was estimated from their gas/liquid density and chemical composition.

misconception that today's front-runners for H_2 storage in materials are metal hydride systems.[37] Indeed, group 3 COFs demonstrate one of the best performances in the class of physisorption materials, approaching the 2010 DOE system target at 77 K. More importantly, the comparable H_2 uptake capacities of the group 3 COFs and MOFs indicate that H_2 uptake capacity is independent of the composition of the structure's backbone and that design of high-affinity sites by metal doping is promising for enhancing H_2 storage performance at ambient temperature.[38]

Room-Temperature Methane Storage in COFs. The interest in natural gas as an alternative fuel has grown considerably.[29,39] Methane is the primary component of natural gas, and it is cleaner than petrol, provides more energy because of its higher hydrogen-to-carbon ratio, and has lower carbon emission. Methane is also abundant and inexpensive compared to conventional fossil fuels, such as gasoline and diesel. However, in order to produce compact automobiles with a driving range of several hundred miles, an effective and safe on-board storage system needs to be achieved. The current storage target set by DOE is 180 cm^3(STP) cm^{-3} at 35 bar, which is comparable to the energy density of compressed natural gas at 250 bar.[39b] For a porous framework to achieve the DOE targets, it must satisfy the following requirements: significant adsorption capacity, efficient charge/discharge rate, high hydrophobicity, moderate adsorption enthalpy, and high heat capacity.[40] Considering the chemical composition (without metals) and pore structure of COFs, it is likely that most of the technical barriers described above can be overcome by modification of the COFs; this is supported by simulation data.[30,41] Here we have undertaken adsorption studies to evaluate the performance of COFs using high-pressure gravimetric instruments.

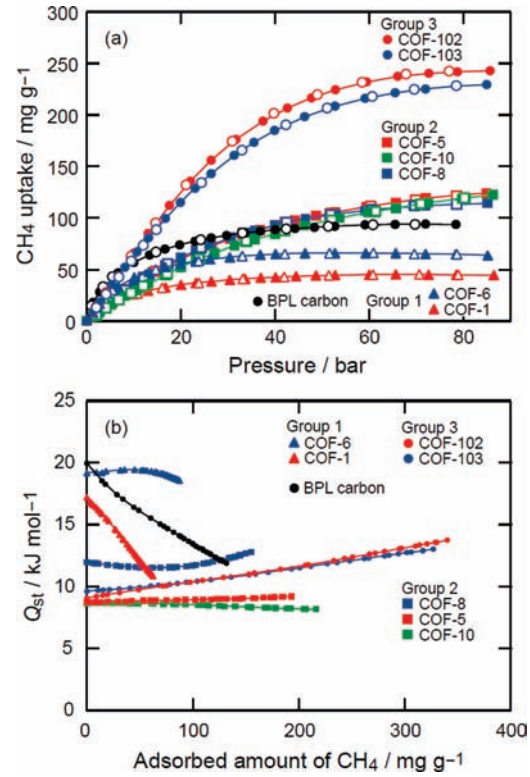

Figure 6. (a) High-pressure CH_4 isotherms for COFs measured at 298 K. (b) Coverage dependency of adsorption enthalpies for COFs. Data for BPL carbon are shown for comparison.

The methane isotherms are shown in Figure 6a and the data summarized in Table 1. The uptake capacity of COFs for methane at room temperature and 70 bar varies according to the porosity of the COF groups: group 1 up to 10 wt %, group 2 between 10 and 15 wt %, and group 3 above 20 wt %. Figure 6 compares CH_4 isotherms for COFs at 298 K and BPL carbon, a material with comparable properties commonly used as an adsorbent. It is clear the COFs exceed BPL carbon in their capacity for methane. The CH_4 uptake values for group 1 COFs, COF-1 and COF-6, at 298 K are estimated to be 44 and 68 mg g^{-1} with saturation pressures of 66 and 50 bar, respectively (Table 1). A superior CH_4 uptake without saturation is observed for the group 2 COFs: 127 mg g^{-1} for COF-5, 114 mg g^{-1} for COF-8, and 124 mg g^{-1} for COF-10. The curvature of the three isotherms implies that larger pore diameters need higher pressure to reach saturation. The isotherms for the group 3 COFs are saturated at approximately 70 bar, with maximum uptake values exceeding 20 wt %. The gravimetric uptakes at 35 bar for COF-102 (187 mg g^{-1}) (Table 1) and COF-103 (175 mg g^{-1}) are higher than those reported for zeolites (31−82 mg g^{-1}),[29] mesoporous silicas (14−65 mg g^{-1}),[29] MOFs (160 mg g^{-1}),[4a,7a] and the majority of activated carbons,[29] nearly the same as those of the high surface area carbons (211 mg g^{-1} for Maxsorb and 250 mg g^{-1} for chemically activated anthracite taken at 293 K),[29,42] but slightly lower than that of PCN-14 (253 mg g^{-1} at 290 K).[7h]

To evaluate the potential deployment of COFs in fuel canisters, the absolute adsorbed amounts in volumetric units (g L^{-1}) were estimated from experimental data (surface excess

(37) Sanderson, K. *Nature* **2007**, *448*, 746–748.
(38) (a) Han, S. S.; Goddard, W. A. *J. Am. Chem. Soc.* **2007**, *129*, 8422–8423. (b) Choi, Y. J.; Lee, J. W.; Choi, J. H.; Kang, J. K. *Appl. Phys. Lett.* **2008**, *92*, 173102.
(39) (a) Wegrzyn, J.; Gurevich, M. *Appl. Energy* **1996**, *55*, 71–83. (b) Burchell, T.; Rogers, M. *SAE Tech. Pap. Ser.* **2000**, 2000−01–2205.
(40) Lozano-Castelló, D.; Alcañiz-Monge, J.; De la Casa-Lillo, M. A.; Cazorla-Amorós, D.; Linares-Solano, A. *Fuel* **2002**, *81*, 1777–1803.
(41) (a) Garberoglio, G. *Langmuir* **2007**, *23*, 12154–12158. (b) Yang, Q.; Zhong, C.; Chen, J.-F. *J. Phys. Chem. C* **2008**, *112*, 1562–1569. (c) Babarao, R.; Jiang, J. *Langmuir* **2008**, *24*, 6270–6278. (d) Garberoglio, G.; Vallauri, R. *Microporous Mesoporous Mater.* **2008**, *116*, 540–547.
(42) (a) Celzard, A.; Fierro, V. *Energy Fuels* **2005**, *19*, 573–583. (b) Celzard, A.; Albiniak, A.; Jasienko-Halat, M.; Marêché, J. F.; Furdin, G. *Carbon* **2005**, *43*, 1990–1999.

mass) and bulk density of CH_4.[32] In the volumetric units, CH_4 uptake, similarly to that of H_2, increases in the order of increasing pore size, indicating that a large pore volume is necessary to demonstrate high gas storage capacity. The uptake for COF-102 is estimated to be 97 and 138 g L^{-1} at 35 and 70 bar, corresponding to 136 and 193 cm^3 cm^{-3}, respectively. Remarkably, CH_4 uptake at 35 bar is roughly 4 times larger than bulk CH_4 density at the same temperature and pressure. The values in cm^3 cm^{-3} units for COF-102 are well within the realm of the DOE target of 180 cm^3 cm^{-3} at 35 bar. It should be noted that the contribution of the packing factor of COF samples is important to determine practical uptake in a canister. The packing density is influenced by both shape and size of the materials and usually is below unity, although these numbers for COFs are not available here. Indeed, the actual volumetric uptake is 20−30% smaller compared to the present data if the packing density is 0.7.[17,43]

The reason for the outstanding CH_4 uptake of the group 3 COFs can be gleaned from the analysis of the high-pressure isotherms at 273 and 298 K. For the estimation of the differential adsorption enthalpy, a fitting curve for the isotherms was obtained from the virial expansion with the same temperature-independent parameters as was done for the case of low-pressure H_2 adsorption presented in Figure 3b. However, for methane adsorption enthalpy there are two new aspects to consider: (1) the absolute adsorbed amounts of CH_4 were used in order to avoid having an artificially negative Q_{st} value,[44] and (2) the pressure was converted to fugacity in order to ignore nonideality of CH_4 under the given conditions. It is possible to obtain reasonable Q_{st} values mathematically if the fitting error is small. However, here we only use these data to demonstrate a general trend for the coverage dependencies of the adsorption enthalpy, because (i) the data conversion process from surface excess to absolute adsorbed amounts includes several assumptions and (ii) more than three temperatures are preferable for reliable calculations.

The estimated isosteric heats of adsorption for COFs are shown graphically in Figure 6b. As expected, the behavior of the differential enthalpy curves is distinctive for each COF. From these plots, it can be seen that the group 1 COFs have larger Q_{st} values than group 2 COFs at low coverage. Additionally, COF-1 shows a gradual decrease in Q_{st} as a function of the amount adsorbed, while COF-6 has large Q_{st} values. Given the high Q_{st} values observed for COF-6, it can be said that smaller cylindrical pores of diameter less than 10 Å are preferable for the storage of CH_4 molecules.

Initial Q_{st} values for the group 2 materials are similar with the exception of COF-8, where the heat of adsorption for COF-8 increases in the high-coverage region. These results are consistent with the similar CH_4 and H_2 uptake behaviors observed under the experimental conditions studied. Considering that the CH_4−adsorbent interactions for the group 2 COFs in the low-coverage region should be analogous due to their functional similarity, the difference in the profile of the Q_{st} curves is attributed to the pore diameter. Indeed, for layered carbon sheets, it is predicted that attractive potential created by the facing pore walls decreases very rapidly with distance and that it becomes almost a simple isolated surface if the distance is larger than 30 Å.[42a,45] Consequently, the diameter of the micropores must be 11−11.5 Å for utilization of the potential wall of the adsorbents.[45,46] Although cylindrical pores may have slightly different optimized conditions,[47] it is likely that adsorbed CH_4 molecules interact with adsorptive CH_4 to increase the total uptake. If a pore diameter of 11−11.5 Å provides an ideal adsorption environment, then group 3 COFs should be good candidates for CH_4 storage since the pore size distribution of these COFs (based on DFT calculations and the Ar isotherms measured at 87 K) is almost the same as the optimized pore size obtained from simulation calculations.[10b] However, the estimated Q_{st} values at low coverage indicate that weaker adsorbate−adsorbent interactions are present in the group 3 COFs. In other words, cooperative interactions between CH_4 molecules lead to a slight incremental increase of the Q_{st} value as a function of the amount adsorbed.[48]

Several important points should be made regarding the moderate Q_{st} values observed for the group 3 COFs. Large Q_{st} values are not necessarily as desirable as an increase in adsorption equilibration time and thus lead to longer fueling time; for example, the equilibration time for BPL carbon is almost 10 min, while that for COF-102 is 3−5 min. Thus, a Q_{st} value of 20 kJ mol^{-1} (found for carbon) may be too high to have complete CH_4 charge/discharge processes within several minutes.[40] Second, the deliverable amount of CH_4 must be considered: strong binding energy is preferable to store a large amount of CH_4 at low pressure, and the difference between stored and delivered amounts may be significant.[42b] Finally, a more exothermic adsorption process will cause a greater increase in the temperature of the system. The steep temperature increment in a canister due to the undissipated heat should prevent CH_4 uptake processes,[40,46a] resulting in a decreased CH_4 capacity. Taking these factors into account, the best conditions for the utilization of group 3 COFs as CH_4 adsorbents would be 150 bar at room temperature, where the amount of CH_4 delivered exceeds 200 cm^3 cm^{-3}.

High-Pressure Carbon Dioxide Adsorption in COFs. The emission of CO_2 due to the combustion of fossil fuels is one of the major sources for the accumulation of CO_2 in the atmosphere. To stabilize atmospheric CO_2 levels, it is necessary to develop CO_2 capture and sequestration technologies (i.e., short- and long-term CO_2 capture).[49] The capture and separation of CO_2 can be achieved by using solvents, cryogenic techniques, and solid sorbents.[50] To date, most of the processes in large-scale operations are performed by amine-based wet scrubbing systems (i.e., postcombustion CO_2 capture by chemisorption),[51]

(43) Strictly speaking, adsorption on the external surfaces of samples needs to be considered. Although the external surface area is estimated by N_2/Ar isotherms, the thickness of the adsorbed layer and density of adsorbate are uncertain because the adsorbed amount on the external surface cannot be easily derived with high accuracy. Since the external surface area of COFs is less than 10% of the internal surface area, we do not consider this effect in this study.

(44) Salem, M. M. K.; Braeuer, P.; Szombathely, M. v.; Heuchel, M.; Harting, P.; Quitzsch, K.; Jaroniec, M. *Langmuir* **1998**, *14*, 3376–3389.

(45) Tan, Z.; Gubbins, K. E. *J. Phys. Chem.* **1990**, *94*, 6061–6069.

(46) (a) Matranga, K. R.; Myers, A. L.; Glandt, E. D. *Chem. Eng. Sci.* **1992**, *47*, 1569–1579. (b) Chen, X. S.; McEnaney, B.; Mays, T. J.; Alcaniz-Monge, J.; Cazorla-Amoros, D.; Linares-Solano, A. *Carbon* **1997**, *35*, 1251–1258.

(47) Cracknell, R. F.; Gordon, P.; Gubbins, K. E. *J. Phys. Chem.* **1993**, *97*, 494–499.

(48) Llewellyn, P. L.; Maurin, G. *C. R. Chimie* **2005**, *8*, 283–302.

(49) (a) Holloway, S. *Energy* **2005**, *30*, 2318–2333. (b) Arenillas, A.; Smith, K. M.; Drage, T. C.; Snape, C. E. *Fuel* **2005**, *84*, 2204–2210.

(50) Xu, X.; Song, C.; Miller, B. G.; Scaroni, A. W. *Fuel Process. Technol.* **2005**, *86*, 1457–1472.

(51) (a) Figueroa, J. D.; Fout, T.; Plasynski, S.; McIlvried, H.; Srivastava, R. D. *Int. J. Greenhouse Gas Control* **2008**, *2*, 9–20. (b) Li, F.; Fan, L.-S. *Energy Environ. Sci.* **2008**, *1*, 248–267.

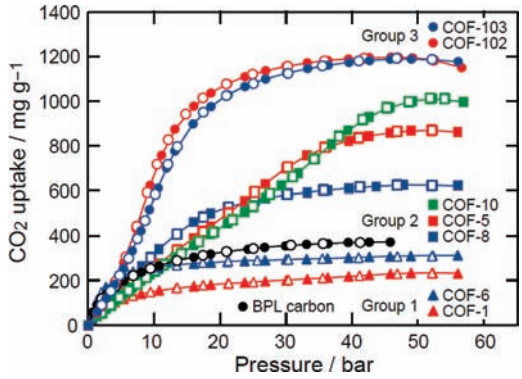

Figure 7. High-pressure CO_2 isotherms for COFs measured at 298 K. Data for BPL carbon are shown for comparison.

because low CO_2 partial pressure and high flue gas temperature (50−120 °C) require strong interaction with CO_2.[49b] However, these processes suffer from high regeneration energy, large equipment size, solvent degradation and equipment corrosion.[50] Therefore, adsorption separation is considered to be a more promising method for cost-effective CO_2 recovery. Recently, two novel technological pathways have been proposed for CO_2 capture systems; precombustion capture and oxy-combustion.[51] Since CO_2 concentrations in these gas streams are much higher than flue gas streams in the postcombustion capture, many limitations in state-of-the-art amine-based systems can be resolved in combination with highly porous solids. Considering that the functionalities of the COFs can be introduced by either design of their organic building blocks or by postsynthesis reactions, we sought to demonstrate their CO_2 uptake capacities as storage materials.

High-pressure CO_2 isotherms for all the COFs were collected and are presented in Figure 7 and Table 1. We find that their surface excess mass uptake and their saturation pressures are sensitive to the structure of the COFs. The CO_2 adsorption isotherms for COF-1, -6, and -8 have a typical type I profile while the uptakes increase monotonically. In contrast, the COF-5, -10, -102, and -103 show sigmoidal isotherms, especially at 273 K.[17] Isotherms for groups 1 and 3 COFs are saturated at a pressure of 35 bar or lower, which is in sharp contrast to the saturation pressure for group 2 COFs (ca. 50 bar). The relationship between the pore diameter and saturation pressure of COFs is similar to that of MOFs,[5] indicating that gas adsorption behavior in COFs is substantively the same as that in MOFs. With regard to the adsorbed amount of CO_2, the surface excess masses increase in the order of group 1 < group 2 < group 3 COFs. The saturation uptakes for group 3 COFs (1200 and 1190 mg g^{-1} for COF-102 and -103, Table 1) are larger than that for MOF-5 (970 mg g^{-1}), carbon materials (420 and 370 mg g^{-1} for Norit RB2 and BPL carbon, respectively), and zeolites (220−350 mg g^{-1}).[5a,7f,52] The high CO_2 storage capacity should be applicable to the short-term CO_2 storage and transport of CO_2, although it is lower than those for MOF-177 and NH_4F-treated MIL-101(Cr) (1490 and 1760 mg g^{-1}, respectively).[5a,7f] However, COF-6, possessing a smaller pore diameter, outperforms other COFs at 273 K and 1 bar (85 cm^3 g^{-1}), a behavior deemed important for the selective capture of CO_2.[17]

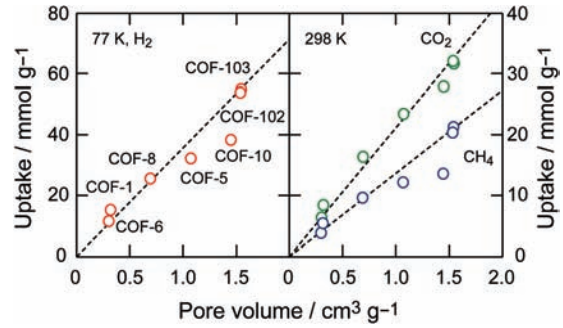

Figure 8. Relationship between absolute gas uptake and pore volume of COFs estimated from Ar isotherms. The regression lines based on the uptakes for COF-1, -6, -8, -102, and -103 are overlaid. Red, blue, and green circles represent the uptakes of H_2 (77 K, 70 bar), CH_4 (298 K, 70 bar), and CO_2 (298 K, 50 bar), respectively.

Capacities as a Function of Pore Size. From CO_2, H_2, and CH_4 uptake behavior in COF materials, it is likely that the intrinsic surface area (or pore volume) plays a critical role in determining the total capacity of gas storage. To clarify this point, absolute uptakes of these gases in millimoles per gram were plotted against the total pore volumes estimated from the DR plots for Ar isotherms (Figure 8). As expected, larger pore volume compounds are advantageous for storing a greater number of guest molecules under the given conditions. These trends are supported by several simulation calculations.[33,53] However, in larger pore materials of COF-5 and COF-10, absolute uptakes of H_2 and CH_4 show small deviations from those of other COFs having smaller pores (microporosity).[54] The boundary of the deviation is seen between COF-8 and COF-5, and this boundary is in accordance with the boundary between micro- and mesopore regions (20 Å is the IUPAC recommendation).[23] These results strongly indicate that the micropore is a prerequisite to increase gas uptake densities as a linear function of the total pore volumes.

Concluding Remarks. We have shown that COFs, a new class of porous crystals, have high capacities for hydrogen, methane, and carbon dioxide. They compare favorably with the most common carbon materials, zeolites, mesoporous solids, and MOFs, an aspect that places them firmly among such useful porous materials.

Acknowledgment. Funding was provided by the DOE (DEFG0-206ER15813) and BASF (Ludwigshafen, Germany). We are grateful to Dr. H. M. El-Kaderi for synthesis of 2D COFs and COF-103, Dr. J. R. Hunt for synthesis of COF-102, and Prof. M. O'Keeffe (Arizona State University) for his invaluable input and continued interest.

Supporting Information Available: N_2, Ar, H_2, CH_4, and CO_2 isotherms for COFs, relationship of pore volumes, effect of packing density on absolute adsorbed amounts, buoyancy correction for adsorbed layer. This material is available free of charge via the Internet at http://pubs.acs.org.

JA9015765

(52) (a) Cavenati, S.; Grande, C. A.; Rodrigues, A. E. *J. Chem. Eng. Data* **2004**, *49*, 1095–1101. (b) Bourrelly, S.; Maurin, G.; Llewellyn, P. L. *Stud. Surf. Sci. Catal.* **2005**, *158*, 1121–1128.

(53) Babarao, R.; Jiang, J. *Energy Environ. Sci.* **2008**, *1*, 139–143.

(54) This section shows that the absolute H_2 uptake at 77 K is directly proportional to the absolute methane uptake at 298 K in the high-pressure region. This diagnostic relationship is useful to assess whether high-pressure measurements are properly done, because the literature is replete with suspicious H_2 adsorption isotherms.[17]